Indian Journal of Chemical Technology
Vol. 33, May 2026, pp. 391-400
DOI: 10.56042/ijct.v33i3.20751

Comparative analysis of humic acid, lignin and lignite-based hydrogels for methylene blue dye removal

Manu Nandal, Devendra Kumar & Rajinder K. Gupta*

Department of Applied Chemistry, Delhi Technological University, Delhi, India

*E-mail- rkg67ap@yahoo.com

Received 17 June 2025; accepted 24 March 2026

This study investigates the application of hydrogels incorporating natural polymers - ammonium humate, lignosulfonate, and ammonium lignite to adsorb methylene blue (MB) from aqueous solutions. The hydrogels were synthesized via free radical polymerization and characterized using FTIR, ^{13}C-NMR, SEM, TGA, and XRD. The synthesized hydrogels demonstrated exceptional swelling capabilities. The influence of various parameters, including adsorbent amount (0.1-0.4 g), temperature (293.15-323.15 K), and initial dye concentration (5-20 mgL^{-1}) on MB removal efficiency was systematically evaluated using the Taguchi method. Under optimized conditions, HA-g-SAH achieved a maximum removal efficiency of 93.7% ±1.1% at 323.15 K, significantly outperforming LS-g-SAH (92.4% ±1.3%), Lt-g-SAH (82.4 ±1.4%), and the control (ctrl) hydrogel (67.9 ±0.9%). According to ANOVA results, the change of biopolymer proved to be an effective factor in the improved dye removal efficiency of hydrogels. Thermodynamic parameters (ΔG°, ΔH°, and ΔS°) were evaluated to assess the temperature effect on adsorption. The adsorption isotherm data were analyzed by applying the Langmuir and Freundlich models. The findings highlight the effectiveness of natural polymer-based hydrogels as sustainable and efficient adsorbents for removing dyes from wastewater.

Keywords: Adsorption Isotherms, Humic acid, Hydrogel, Lignin, Lignite, Methylene blue

Introduction

Synthetic dyes are widely applied across multiple industries such as textiles, pharmaceuticals, and food manufacturing. However, a significant portion estimated at around 80% of dye-laden effluents is frequently discharged without adequate treatment into natural water systems or used for agricultural irrigation, posing serious risks to environmental and public health[1]. Synthetic dye effluents are highly toxic due to the presence of harmful substances such as sulfur compounds, vat dyes, nitrates, acids, surfactants, enzymes, chromium, and heavy metals like lead, cadmium, and mercury, posing serious risks to living organisms[2]. The colour of dyes causes aesthetic damage to the water bodies and also prevents passing of light through water, which reduces the photosynthetic activity by decreasing dissolved oxygen levels, which collectively disrupt aquatic ecosystems[3].

Methylene blue, a widely used dye, contributes significantly to environmental pollution due to its toxicity. Its presence can interfere with photosynthesis and cause severe eye burns, potentially leading to permanent eye damage in both humans and animals[4]. Additionally, exposure to MB in humans can result in adverse effects such as tissue necrosis, cyanosis, jaundice, vomiting, increased heart rate, and other health complications.[5] Consequently, removing MB from industrial wastewater is a pressing ecological concern. The high solubility of dye in water makes it difficult to remove them by conventional methods[6]. Both destructive and non-destructive techniques have been effectively utilized for dye removal from wastewater. Non-destructive approaches include ion exchange[7], chemical oxidation[8], ozone treatment [9], membrane separation [10], and coagulation[11] each presenting specific advantages and limitations. Among the various strategies reported in the literature, adsorption has emerged as a particularly efficient method for eliminating dyes from industrial effluents[12].

Among the various treatment methods investigated for the removal of dyes from industrial effluents, adsorption has been extensively studied and is regarded as one of the most effective techniques for removing dyes from industrial wastewater due to its simplicity, cost-effectiveness, and high removal capacity[13]. Hydrogel, a polymeric material, stands out

for its exceptional hydrophilicity, mechanical properties, and high porosity, allowing it to absorb water a thousand times its original size[14]. pollutant adsorption, sensing, and tissue engineering. These functionalities can be tailored by modifying the chemical composition and structural properties of the hydrogel matrix.

Owing to their high water content, porous nature, and inherent biocompatibility, hydrogels have been extensively utilized in applications such as drug release[15–19], pollution adsorption[13,20], sensors [21,22] and tissue engineering [23,24]. Due to their crosslinked polymer networks and the presence of reactive functional groups, these materials have shown significant potential for the removal of dyes, particularly MB[20,25–27].

Humic acid, lignin, and lignite are natural polymers that are highly suitable for constructing adsorbent hydrogels for water purification due to their abundance and biodegradable nature. Also, hydrogels reinforced with natural polymers possess excellent mechanical properties[28]. Humic acid is a large organic polymer found in soil and water. It has chelating properties and is important for soil and plant health. In literature, the direct utilization of this natural polymer for adsorption applications is extensively reported. Lignite, or brown coal, is well-known for its adsorptive properties. Numerous investigations have identified lignite as a potential adsorbent for the removal of heavy metals, dyes, and various organic contaminants from wastewater[29–32]. A biodegradable hybrid hydrogel composed of acrylic acid, acrylamide, sodium acrylate, and sodium humate was developed by Singh *et al*. for MB and crystal violet adsorption. The hydrogel demonstrated enhanced adsorption performance in its swollen state, with sodium humate (2.40 wt%) contributing significantly to both swelling behavior and overall adsorption efficiency[33]. Yu *et al*. [34] synthesized superabsorbent hydrogels by grafting acrylic acid (AA) onto a lignosulfonate (LS) matrix. The resulting LS-g-AA hydrogel exhibited a maximum equilibrium adsorption capacity for MB of 2013 mg g^{-1}.

All three natural polymers- humic acid, lignin and lignite- contain carboxylic acid and phenolic moieties that could enhance the cationic dye adsorption capability. Also, owing to their polyfunctionality, ammonium salts of humic acid, lignite, and lignosulfonate sodium salt can be grafted onto acrylic acid to synthesize hydrogels. Keeping this in view, the study focuses on the application of ammonium humate, lignosulfonate and ammonium lignite-based hydrogels (HA-g-SAH, LS-g-SAH, and Lt-g-SAH) for adsorption of MB from water. The influence of factors like temperature, initial dye concentration, contact time, and adsorbent amount was systematically investigated to enhance the MB removal efficiency (%R) of HA-g-SAH, LS-g-SAH, Lt-g-SAH, and ctrl hydrogels. Taguchi experimental design was adopted for analyzing the adsorption factors having the most significant influence. The optimized swelling duration of all hydrogels from our previous study[28] has been employed as the contact time to obtain the best results. The adsorption isotherm study has also been carried out, where the dye %R of hydrogels is fitted to Langmuir and Freundlich models. As per the present literature, no such study has been conducted that employs these hydrogels together and presents a comparative analysis of hydrogels' dye %R, comparing them to non-grafted ctrl hydrogel. The findings suggest that the synthesized hydrogel demonstrates enhanced performance and high efficacy in the removal of MB from wastewater.

Experimental Section

Methods

Swelling Study

Swelling experiments were performed on varied weight of biopolymer of HA-g-SAH, LS-g-SAH, Lt-g-SAH, and ctrl hydrogels at 37°C in distilled water to optimize the best compositions for the adsorption experiment. Initially, the weight of dried hydrogel discs was measured (W_d). At fix time intervals, the hydrogel discs were taken out of water. Excess water present at surface was absorbed using filter paper, and the hydrogel discs were reweighed (W_0). The swelling study was carried out in triplicate.

The swelling index (SI) was determined utilizing Eq. (1):

$$SI(gg^{-1})=\frac{W_o-W_d}{W_d} \quad \text{... (1)}$$

MB Adsorption experiment mechanism

The experiments were designed using the Taguchi method with standard orthogonal array tables. The Taguchi approach is an efficient optimization strategy that minimizes the influence of uncontrollable variables by employing a limited set of experimental

runs[35]. The L16 orthogonal array facilitates the identification of optimal control parameters while significantly reducing the total number of experiments required[36].

The influence of the variation of the amount of adsorbent (0.1-0.5 g), temperature (293.15 - 323.15 K) and contact time (HA-g-SAH- 47 h, LS-g-SAH - 37 h, Lt-g-SAH -34 h, and ctrl -31 h, based on their optimized swelling duration[28]) were studied on the adsorption of initial MB concentration ranging from 5-20 mg L^{-1}. After removing hydrogels, the unabsorbed MB content in the aqueous solution was determined by MB's absorption on UV-visible spectrophotometer at 664 nm using a UV1800 Shimadzu spectrophotometer[37]. The %R of MB was determined using Eq. (2):

$$\% \text{ R} = \frac{C_o - C_e}{C_o} \text{X } 100 \quad \text{... (2)}$$

'q_e' (mg g^{-1}) denotes the adsorption capacity of HA-g-SAH, LS-g-SAH, Lt-g-SAH, and ctrl, hydrogels. It wascalculated through Eq. (3):

$$q_e = \frac{C_0 - C_e}{m} V \quad \text{… (3)}$$

C_e and C_0 (mg L^{-1}) denote the equilibrium and initial concentrations of MB, respectively. V (L) represents the solution volume, while m (g) corresponds to the mass of the hydrogels—HA-g-SAH, LS-g-SAH, Lt-g-SAH, and the ctrl—used in the adsorption experiments.

Results and Discussion

Swelling study

Table 1 demonstrates the swelling behaviour of the HA-g-SAH, LS-g-SAH, Lt-g-SAH and ctrl hydrogels studied in distilled water. The results indicate that the SI is highly influenced by the weight of biopolymers (Ammonium Humate/Lignosulfonate/Ammonium lignite). HA-g-SAH hydrogel exhibited the highest swelling in distilled water (280.92 g g^{-1}) in 47 h. It was followed by LS-g-SAH (258.33 g g^{-1}) in 37 h and Lt-g-SAH (187.4 g g^{-1}) in 34 h. Ctrl hydrogel had the lowest SI of 142.58 g g^{-1} in 31 h. Thus, hydrogel formulation no's 5, 4, and 5 of Ammonium Humate, Lignosulfonate, and Ammonium lignite, respectively, were found to have the highest swelling and consequently used for the swelling and adsorption experiments.

The observed swelling trend also correlates well with the adsorption performance of the hydrogels towards MB. Hydrogels with higher SI are expected to provide a more expanded polymeric network and increased internal free volume, which facilitates easier diffusion of dye molecules into the hydrogel matrix and improves accessibility to available functional groups. For instance, HA-g-SAH and LS-g-SAH exhibited high (280.92 g g^{-1} and 258.33 g g^{-1}, respectively) and correspondingly achieved higher %R of MB (93.7% ± 1.1% and 92.4% ± 1.3%). In comparison, Lt-g-SAH with a lower SI (187.4 g g^{-1}) showed moderate removal efficiency (82.4% ± 1.4%), which ctrl hydrogel (142.58 g g^{-1}) with lowest SI displayed lowest removal efficiency (67.9% ± 0.9%). This quantitative relationship suggests that the enhanced swelling behaviour contributes significantly to improved adsorption by enabling greater dye diffusion and interaction with functional groups present within the hydrogel network.

MB adsorption and isotherm study

The %R of MB obtained from varying the adsorbent amount (0.1-0.5 g), temperature (293.15 - 323.15 K), and initial MB concentration (5 - 20 mg L^{-1}) on the adsorption of MB is reported in Table 2. Fig. 1a represents the ANOVA box plots for Table 1, representing %R of MB with HA-g-SAH, LS-g-SAH, Lt-g-SAH and ctrl hydrogel. The ANOVA results indicated that the %R of HA-g-SAH, LS-g-SAH, Lt-g-SAH, and Ctrl were statistically significant, as the observed P-value (F-test) was less than 0.05. This suggests a probability of less than 5% for the null

Table 1 — Swelling study analysis of HA-g-SAH, LS-g-SAH, Lt-g-SAH and ctrl hydrogels

Observation	Ammonium Humate/Lignosulfonate/ Ammonium lignite (g)	SI (gg^{-1})			
		HA-g-SAH	LS-g-SAH	Lt-g-SAH	Ctrl
1	0.0	-	-	-	142.58
2	0.05	136.66	121.78	95.64	-
3	0.1	201.45	170.56	113.87	-
4	0.2	267.56	258.33	159.22	-
5	0.3	280.92	230.45	187.4	-
6	0.4	228.12	187.34	152.72	-
7	0.5	173.45	136.45	135.65	-

Table 2 — Taguchi L16 design table for HA-g-SAH,LS-g-SAH, Lt-g-SAH and ctrl hydrogel

Observations	Adsorbent (g)	Temperature (K)	Initial dye conc. (mg L^{-1})
Obs1	0.1	293.15	5
Obs2	0.1	303.15	10
Obs3	0.1	313.15	15
Obs4	0.1	323.15	20
Obs5	0.2	293.15	10
Obs6	0.2	303.15	5
Obs7	0.2	313.15	20
Obs8	0.2	323.15	15
Obs9	0.3	293.15	15
Obs10	0.3	303.15	20
Obs11	0.3	313.15	5
Obs12	0.3	323.15	10
Obs13	0.4	293.15	20
Obs14	0.4	303.15	15
Obs15	0.4	313.15	10
Obs16	0.4	323.15	5

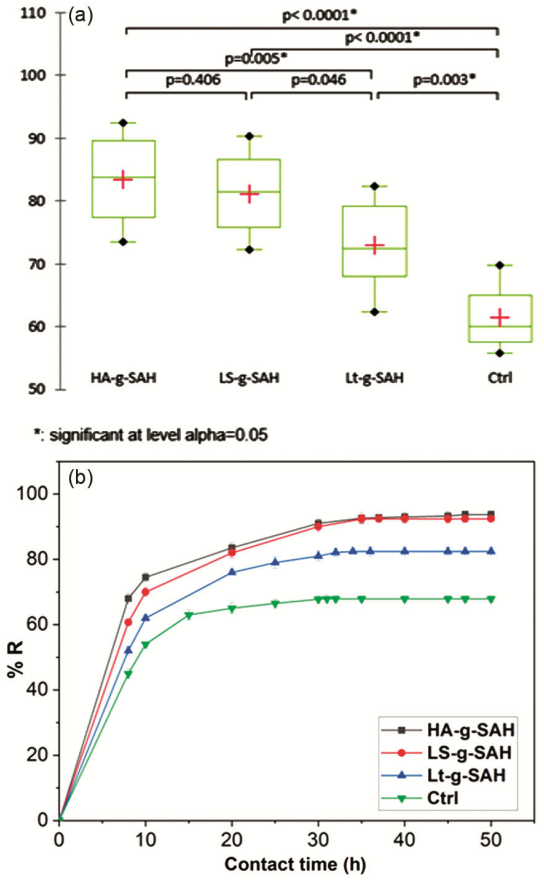

Fig. 1 — ANOVA box plots for Table 1

hypothesis to be valid. Consequently, the observed variations are attributed to the differences in the biopolymers used during hydrogel synthesis.

Effect of variation in the amount of adsorbent on %R of MB

The amount of HA-g-SAH, LS-g-SAH, Lt-g-SAH and ctrl hydrogel used were 0.1 to 0.4 g per 100 mL of 20 mg L^{-1} MB at 323.15 K and their respective optimized contact time.It can be observed from Fig. 2a that the %R demonstrated a distinct sigmoidal pattern with increasing adsorbent amount. At 0.1 g, HA-g-SAH achieved 59.5% ± 1.0% %R, with LS-g-SAH showing similar performance at 57.7% ± 2.0%. A significant enhancement occurred between 0.2 and 0.3 g, where HA-g-SAH and LS-g-SAH reached 92.5% ± 2.2% and 91.4% ± 1.5%, respectively. This sharp increase indicates a critical threshold for optimal adsorption.

At 0.4 g, the systems approached equilibrium, with HA-g-SAH achieving maximum efficiency of 93.7% ± 3.0%, followed by LS-g-SAH (92.4% ± 1.6%), Lt-g-SAH (82.4% ± 2.7%), and ctrl hydrogel (67.9% ± 1.1%). The plateauing effect beyond 0.3 g suggests saturation conditions. The %R is found to be in the order HA-g-SAH > LS-g-SAH > Lt-g-SAH > Ctrl, representing intrinsic differences in adsorption capabilities, with HA-g-SAH's superior performance attributed to humic acid's abundant functional groups and favourable surface characteristics. This analysis identifies 0.3 g as the optimal adsorbent amount, balancing maximum %R with material usage.

Effect of variation in temperature on%R of MB

Fig. 2b shows the adsorption of the dyes onto the HA-g-SAH, LS-g-SAH, Lt-g-SAH, and ctrl hydrogels from temperatures 293.15 K to 323.15 K. Thermodynamic parameters—enthalpy change (ΔH^0), entropy change (ΔS^0), and Gibbs free energy change (ΔG^0)—related to the dye adsorption process were evaluated using the corresponding equations[37].

$$K = \frac{C_0 - C_e}{C_e} \quad \ldots (4)$$

$$\Delta G° = -RTlnK \quad \ldots (5)$$

$$\Delta G° = \Delta H° - T\Delta S° \quad \ldots (6)$$

$$\ln (k) = \frac{\Delta S^0}{R} - \frac{\Delta H^0}{RT} \quad \ldots (7)$$

The symbol K represents the equilibrium constant, while C_e and C_0 represent the equilibrium and initial concentrations of the dye (mg L^{-1}), respectively. The universal gas constant is represented by 'R', and T (K) is the absolute temperature. The van't Hoff plot, depicting ln K versus 1/T (Fig. 2c), was used to determine the standard enthalpy (ΔH^0) and entropy

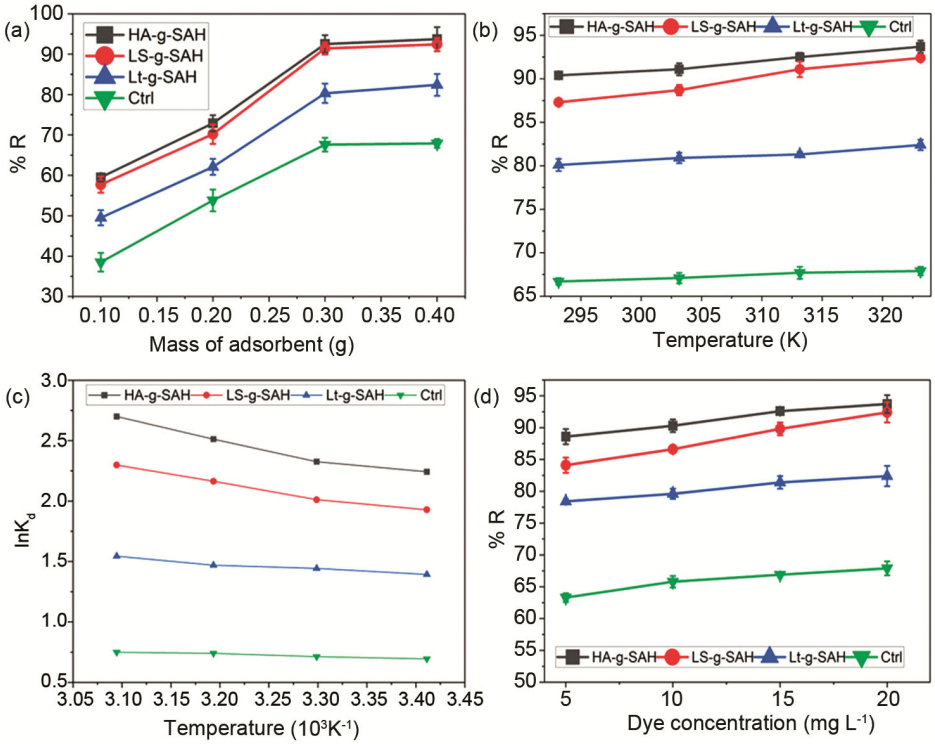

Fig. 2 — Effect of the variation in (a) adsorbent amount (T = 323.15 K, dye conc.= 20 mg L^{-1}), (b) temperature (adsorbent = 0.3 g, dye conc.= 20 mg L^{-1}), (c) van't Hoff plots of ln K_d against 1/T, (d) initial dye concentration (adsorbent= 0.3 g, T= 323.15K and (e) contact time on %R (adsorbent= 0.3 g, T= 323.15K, dye conc.= 20mg L^{-1}) by HA-g-SAH, LS-g-SAH, Lt-g-SAH, and Ctrl hydrogels

Table 3 — Thermodynamic parameters (ΔG°, ΔH° and ΔS°) of MB adsorbed on the HA-g-SAH, LS-g-SAH, Lt-g-SAH and ctrl

Parameter	HA-g-SAH	LS-g-SAH	Lt-g-SAH	Ctrl
ΔG° (kJmol^{-1}) T=293.15 K	-6.02	-5.17	-3.74	-1.86
ΔG° (kJ mol^{-1})T=303.15 K	-6.24	-5.40	-3.87	-1.91
ΔG° (kJ mol^{-1}) T=313.15 K	-6.74	-6.34	-3.94	-1.98
ΔG° (kJ mol^{-1}) T=523.15 K	-7.25	-6.71	-4.14	-2.01
ΔH° (kJ mol^{-1})	12.13	9.89	3.74	1.49
ΔS° (JK^{-1} mol^{-1})	59.86	49.63	24.38	10.89

(ΔS^0) changes derived from the slope ($\frac{\Delta H^0}{R}$) and intercept ($\frac{\Delta S^0}{R}$) of the linear fit.

It can be observed from Fig. 2b that %R increases with temperature (293.15-323.15 K) for all adsorbents, with HA-g-SAH demonstrating superior performance (90.4 ±0.4% to 93.7±0.7%), followed by LS-g-SAH (87.3 ±0.4% to 92.4 ±0.4%), Lt-g-SAH (80.1±0.7% to 82.4 ±0.6%), and ctrl (66.7 ±0.5% to 67.9 ±0.3%).

Table 3 shows that the Gibbs free energy (ΔG°) values are negative and decrease with increasing the temperature, indicating spontaneous adsorption with enhanced favorability at higher temperatures. The progressively more negative ΔG° values with rising temperature indicate enhanced thermodynamic favourability of the adsorption at higher temperatures[38]. The positive ΔH° values further confirm that the adsorption process is endothermic[39]. The positive entropy (ΔS°) for all systems indicates increased solid- interface solution randomness during adsorption, suggesting the release of water molecules from hydrogels during adsorption[40]. The combination of positive ΔH° and ΔS° values, along with negative ΔG° values, suggest that the adsorption process by hydrogels is driven by entropy.

Effect of variation in initial dye concentration on %R of MB

Adsorbate solution concentration also significantly influences the adsorption behaviour of the hydrogel[41]. Thus, the impact of initial MB concentration

(5-20 mg L^{-1}) on %R of MB was investigated using HA-g-SAH, LS-g-SAH, Lt-g-SAH, and ctrl hydrogel with 0.3 g adsorbent amount at 323.15 K. Fig. 2d concluded that %R increased as the initial dye concentration increased for all hydrogels. However, HA-g-SAH demonstrated exceptional performance, with %R increasing from 88.58% ± 1.2% at 5 mg L^{-1} to 93.7% ± 1.4% at 20 mg L^{-1}, indicating optimal adsorbent-adsorbate interactions. LS-g-SAH showed similar behavior but slightly lower efficiency, improving from 84.1% ± 1.2% to 92.4% ± 1.6%. Lt-g-SAH displayed moderate performance, with efficiency increasing from 78.4% ± 0.3% to 82.4% ± 1.6%, while the ctrl hydrogel exhibited the lowest capacity, ranging from 63.3% ± 0.7% to 67.9% ± 1.1%. The consistent performance hierarchy (HA-g-SAH > LS-g-SAH > Lt-g-SAH > Ctrl) and minor standard deviations across all concentrations demonstrate the inherent differences in the adsorption capabilities of all the hydrogels. Also, the gradual improvement in %R with increasing dye concentration suggests that HA-g-SAH, LS-g-SAH, and Lt-g-SAH hydrogels maintain effectiveness under varying pollutant loads, making them suitable for practical wastewater treatment applications.

Effect of variation in contact time on %R of MB

Analyzing contact time is crucial to assess the reaction extent during the adsorption process. Fig. 2e illustrates the influence of contact duration on MB adsorption by HA-g-SAH, LS-g-SAH, Lt-g-SAH, and ctrl hydrogels. The results demonstrated that the adsorption capacity of all hydrogel samples increased progressively over time. Also, a clear progression of MB adsorption is visible through three distinct kinetic phases. During the rapid initial phase spanning the first 10 h, HA-g-SAH demonstrated the highest uptake at 74.5% ±1.4%, followed by LS-g-SAH at 70% ± 1.2%, Lt-g-SAH at 62% ± 0.9%, and the ctrl at 54% ±0.8%. The progressive phase from 10-30 h showed HA-g-SAH and LS-g-SAH reaching approximately 90-91%, while Lt-g-SAH and the ctrl exhibited slower progression, achieving 79% ± 1.7% and 65% ±1.6%, respectively. In the final equilibrium phase, HA-g-SAH reached 93.7% ±1.1% in 47 h, while LS-g-SAH attained 92.4% ±1.3% in 37 h, Lt-g-SAH achieved 82.4% ± 1.4%in 34 h, and the ctrl plateaued at 67.9% ±0.9% in 31 h. Throughout the study, the performance hierarchy remained consistent, with HA-g-SAH performing best, followed by LS-g-SAH, Lt-g-SAH, and the ctrl.

Thus, the present biopolymers (ammonium humate, lignosulfonate sodium and ammonium lignite) significantly increase the adsorption of cationic dye MB due to their ability to form strong electrostatic interactions with the dye molecules having a positive chargeand through their phenolic groups with a negative charge. Since all the modified hydrogels demonstrated superior adsorption properties compared to the ctrl, it may be concluded that the polyphenols act as an attractive surface for the cationic dye to bind to, enhancing the adsorption capacity of their respective hydrogels.

Adsorption isotherms

Adsorption isotherms are valuable tools for understanding how adsorbate (MB) molecules are distributed between the solution phase at equilibrium and the adsorbent surface. Adsorption isotherms offer useful information regarding the affinity and capacity of an adsorbent by characterizing its interaction with the adsorbate. The adsorption behaviour in this study was examined using both Langmuir and Freundlich isotherm models[18].

The Langmuir isotherm model is well-suited for representing monolayer adsorption on a uniform surface. Eqs (8 and 9) defines the Langmuir isotherm's linear forms[42].

$$\frac{q_e}{C_e} = \frac{1}{K_l q_{max}} + \frac{C_e}{q_{max}} \quad \ldots (8)$$

$$\frac{1}{q_e} = \frac{1}{q_{max}} + \frac{C_e}{q_{max} b C_e} \quad \ldots (9)$$

The parameters q_{max} (mg g^{-1}), C_e (mg L^{-1}), q_e (mg g^{-1}) and represent the theoretical maximum adsorption capacity of hydrogels, the equilibrium concentration of MB in solution and the adsorption capacity of hydrogels at equilibrium and, respectively, while K_L(L mg^{-1}) denotes the Langmuir constant. These parameters can be obtained by plotting a linear graph of C_e versus q_e/C_e and calculating the slope and intercept. The dimensionless separation factor (R_L) is an indicator for evaluating the feasibility of a reaction. The R_L values may be interpreted as follows: favourable (R_L values between 0 and 1) or unfavourable (R_L values greater than 1). It is calculated using Eq. (10),

$$R_L = \frac{1}{1+K_l C_i} \quad \ldots (10)$$

where, MB concentration is given by C_i (mg L^{-1}).

The Freundlich isotherm model proposes that adsorbents with heterogeneous surfaces experience

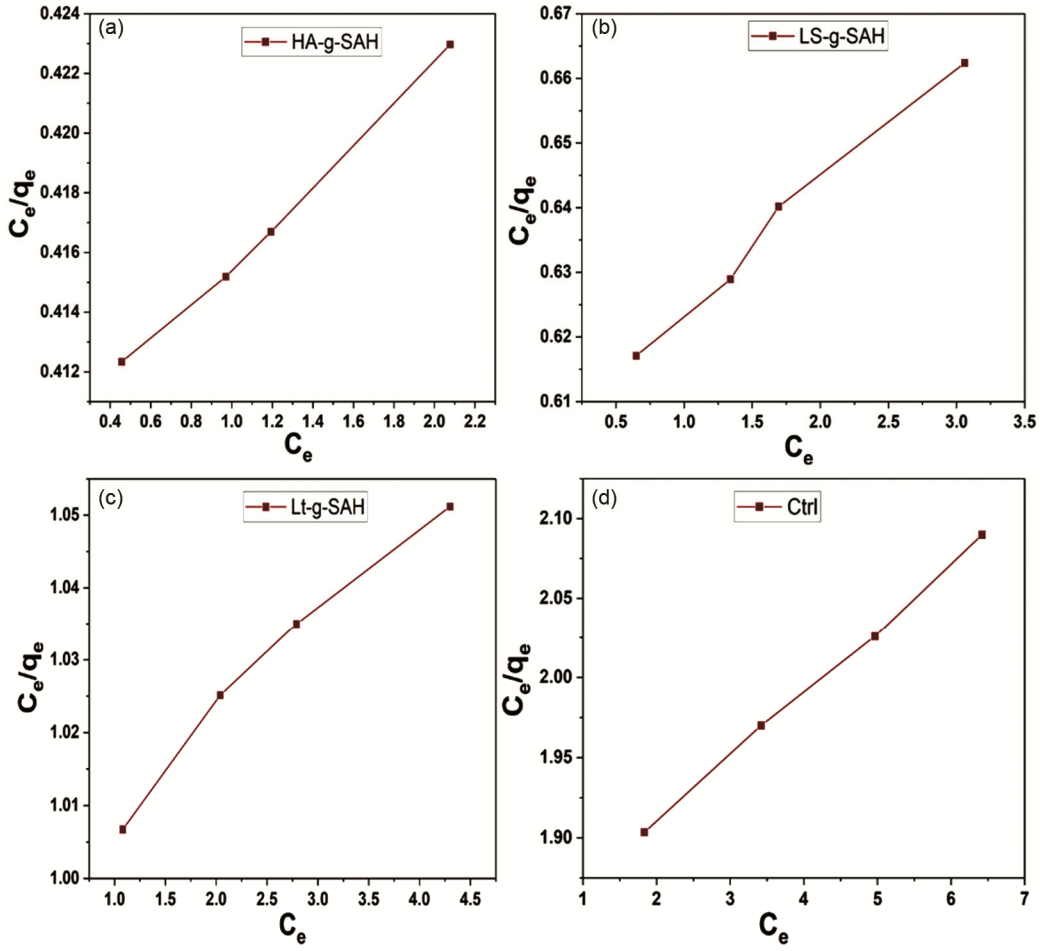

Fig. 3 — Langmuir isotherm graphs of (a) HA-g-SAH, (b) LS-g-SAH, (c) Lt-g-SAH and (d) ctrl hydrogels used for MB adsorption

multilayer adsorption. In the early stages, the more robust binding sites are mainly occupied, and the equilibrium concentration of the adsorbates largely influences the binding strength. The linear Equation for Freundlich isotherm is given by Eq. (11)[43]

$$lnq_e = lnK_f + \frac{1}{n}\ln \quad \text{... (11)}$$

where K_f [(mg g^{-1}) (L mg^{-1})] is the Freundlich constant. It explains binding energy, adsorption capacity, and quantity of MB adsorbed at equilibrium[43]. The '1/n' value indicates the intensity of adsorption or the heterogeneity of the surface. An 'n' value of 1 to 10 indicates a favourable adsorption process. The reliability of an adsorption isotherm model is typically evaluated by fitting experimental data to the corresponding theoretical equations, with the coefficient of determination (R^2) used as a measure of the model's goodness of fit. Fig. 3 and Fig. 4 depict the plots of Langmuir and Freundlich adsorption isotherms, and Tables 4 and 5 present the calculated parameters.

The Langmuir model showed a good fit for all samples, with R^2 values ranging from 0.9168 for the ctrl to 0.9786. From Table 4, the Langmuir constant 'b', which reflects binding energy, was highest for HA-g-SAH (b=0.038), indicating the most substantial adsorption, while the ctrl hydrogel had the lowest b=0.015. The separation factor R_L values for all hydrogels fell within the range of 0 to 1, confirming favourable adsorption, with HA-g-SAH exhibiting the most favourable value (R_L=0.37) and the ctrl hydrogel the least favourable (R_L=0.76).

In the Freundlich model, the R^2 values indicated an excellent fit for all hydrogels. From Table 5, the Freundlich constant 'K_f', which signifies adsorption capacity, was highest for HA-g-SAH (K_f=2.84) and lowest for the ctrl (K_f=1.65), while the adsorption intensity parameter '1/n' ranged from 0.31 for HA-g-SAH to 0.58 for the ctrl, with lower values indicating

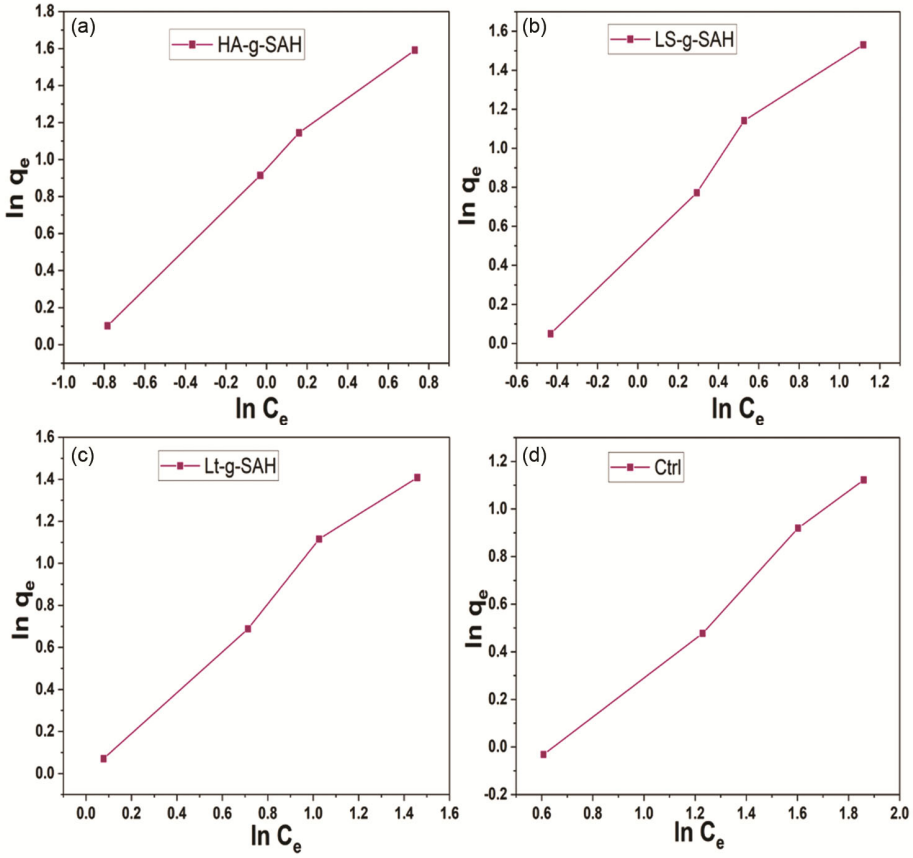

Fig. 4 — Freundlich Isotherm Graph of (a) Ha-g-SAH, (b) LS-g-SAH, (c) Lt-g-SAH, and (d) ctrl hydrogels used for MB adsorption

Table 4 — Isotherms data for Langmuir adsorption isotherm

	R^2	b	R_L
HA-g-SAH	0.9751	0.038	0.37
LS-g-SAH	0.9786	0.024	0.62
Lt-g-SAH	0.9654	0.02	0.69
Ctrl	0.9168	0.015	0.76

Table 5 — Isotherms data for Freundlich adsorption isotherm

Hydrogel	R^2	K_f	1/n
HA-g-SAH	0.9854	2.84	0.31
LS-g-SAH	0.9685	2.52	0.36
Lt-g-SAH	0.9923	2.01	0.42
Ctrl	0.9962	1.65	0.58

more favourable adsorption. These results confirmed that HA-g-SAH is the most efficient adsorbent, demonstrating the highest adsorption capacity and most favourable intensity. LS-g-SAH and Lt-g-SAH also showed good adsorption performance, though slightly less effective than HA-g-SAH, while the ctrl hydrogel exhibited the weakest adsorption characteristics.

Overall, functionalized hydrogels (HA-g-SAH, LS-g-SAH, and Lt-g-SAH) outperformed the ctrl hydrogel, with HA-g-SAH emerging as the most effective adsorbent for MB removal due to its higher binding energy and superior adsorption capacity.

Conclusion

The research successfully demonstrated the application of efficient hydrogel systems incorporating natural polymers for MB removal from aqueous solutions. The comparative analysis revealed that HA-g-SAH exhibited superior performance with a maximum %R of 93.7 ±1.1% at 323.15 K and 0.3 g adsorbent amount, followed by LS-g-SAH (92.4 ±1.3%) and Lt-g-SAH (82.4 ±1.1%), all significantly outperforming the ctrl hydrogel (67.9 ±0.9%). The thermodynamic analysis confirmed the endothermic and spontaneous nature of the adsorption, as indicated by ΔG° values between −7.25 and −1.86 kJ mol^{-1} and ΔH° values in the range of 1.49 to 12.13 kJ mol^{-1}.The Freundlich isotherm model provided the best fit (R^2 values: 0.9854-0.9962), indicating heterogeneous surface adsorption with favourable adsorption intensity parameters (1/n) ranging from 0.31 to 0.58. The enhanced performance of the functionalized hydrogels can be attributed to the presence of

carboxylic and phenolic moieties from the natural polymers, which facilitate strong electrostatic interactions with the cationic dye molecules. The study establishes these natural polymer-based hydrogels as promising candidates for wastewater treatment applications, offering a sustainable solution for dye removal while maintaining high efficiency and environmental compatibility.

Acknowledgement

The authors would like to acknowledge the Department of Applied Chemistry, Delhi Technological University, Delhi, for providing the research facilities to conduct this research.

Conflict of Interest

The authors declare no conflict of interest.

References

1 Lin J, Ye W, Xie M, Seo D H, Luo J, Wan Y & Van der Bruggen B, Environmental impacts and remediation of dye-containing wastewater, *Nat Rev Earth Environ*, 4 (2023) 785.
2 Kant R, Textile dyeing industry an environmental hazard, *Nat Sci*, 4 (2012) 22.
3 Lellis B, Fávaro-Polonio C Z, Pamphile J A & Polonio J C, Effects of textile dyes on health and the environment and bioremediation potential of living organisms, *Biotechnol Res Innov*, 3 (2019) 275.
4 Tan I A W, Ahmad A L & Hameed B H, Adsorption of basic dye using activated carbon prepared from oil palm shell: Batch and fixed bed studies, *Desalination*, 225 (2008) 13.
5 Vadivelan V & Kumar K V, Equilibrium, kinetics, mechanism, and process design for the sorption of methylene blue onto rice husk, *J Colloid Interf Sci*, 286 (2005) 90.
6 Hassan M M & Carr C M, A critical review on recent advancements of the removal of reactive dyes from dyehouse effluent by ion-exchange adsorbents, *Chemosphere*, 209 (2018) 201.
7 Joseph J, Radhakrishnan R C, Johnson J K, Joy S P & Thomas J, Ion-exchange mediated removal of cationic dye-stuffs from water using ammonium phosphomolybdate, *Mater Chem Phys*, 242 (2020) 122488.
8 Dutta S, Gupta B, Srivastava S K & Gupta A K, Recent advances on the removal of dyes from wastewater using various adsorbents: A critical review, *J Mater Adv*, 2 (2021) 4497.
9 Augustowski D, Gala M, Kwaśnicki P & Rysz J, Efficiency boost in dye-sensitized solar cells by post- annealing UV-ozone treatment of TiO_2 mesoporous layer, *Materials*, 14 (2021) 4698.
10 Jirankova H, Mrazek J, Dolecek P & Cakl J, Organic dye removal by combined adsorption-membrane separation process, *Desalin Water Treat*, 20 (2010) 96.
11 Jargalsaikhan M, Lee J, Jang A & Jeong S, Efficient removal of azo dye from wastewater using the non-toxic potassium ferrate oxidation-coagulation process, *Appl Sci*, 11 (2021) 6825.
12 Sivakumar R & Lee N Y, Adsorptive removal of organic pollutant methylene blue using polysaccharide-based composite hydrogels, *Chemosphere*, 286 (2022) 131890.
13 Srivastava A, Manu & Gupta R K, Xanthan gum and lignin grafted chemically crosslinked hydrogels for dye removal: Synthesis, characterization and isotherms studies, *Polym Sci Ser A*, 65 (2023) 725.
14 Manu, Kumar D & Gupta R K, Synthesis, characterization and application of Lignosulphonate-g- poly(sodium acrylate) hydrogel, *Indian J Chem Technol*, 30 (2023) 753.
15 Tanwar M, Rani A & Gupta R K, Synthesis and characterization of carboxymethylated locust bean gum-co-poly(SA)-cl-poly(MBA) pH responsive hydrogel for controlled drug delivery of metformin hydrochloride, *Chem Select*, 8 (2023) e202302525.
16 Tanwar M, Gupta R K & Rani A, Natural gums and their derivatives based hydrogels: In biomedical, environment, agriculture, and food industry, *Crit Rev Biotechnol*, 44 (2024) 275.
17 Kumar J & Purwar R, A Schiff base hydrogel of oxidized okra gum and carboxymethylated chitosan: A biocompatible and biodegradable injectable system for drug delivery in wound care, *Colloid Polym Sci*, 302 (2024) 1923.
18 Kumar J & Purwar R, Self-healing, biocompatible injectable hydrogel based onmultialdehyde moringa oleifera gum and carboxymethyl chitosan: A suitable platform for drug delivery in wound healing application, *Chem Select*, 9 (2024) e202400309.
19 Kumar J & Purwar R, Injectable mesquite gum and carboxymethyl chitosan hydrogel using schiff base crosslinks: A versatile platform for drug delivery in wound care, *Macromol Res*, 32 (2024) 1237.
20 Manu, Kumar D & Gupta R K, Natural polymers-humic acid and lignin based hydrogels: In agriculture, environment and energy storage, *Ind Crops Prod*, 219 (2024) 119029.
21 Ma J, Zhong J, Sun F, Liu B, Peng Z, Lian J, Wu X, Li L, Hao M & Zhang T, Hydrogel sensors for biomedical electronics, *Chem Eng J*, 481 (2024) 148317.
22 Li H, Dai C & Hu Y, Hydrogels for chemical sensing and biosensing, *Macromol Rapid Commun*, 45 (2024) 2300474.
23 Khan M U A, Stojanović G M, Abdullah M F B, Dolatshahi-Pirouz A, Marei H E, Ashammakhi N & Hasan A, Fundamental properties of smart hydrogels for tissue engineering applications: A review, *Int J Biol Macromol*, 254 (2024) 127882.
24 Radulescu D M, Neacsu I A, Grumezescu A M & Andronescu E, New insights of scaffolds based on hydrogels in tissue engineering, *Polymers*, 14 (2022) 799.
25 Zamani-Babgohari F, Irannejad A, Kalantari P M & Khayati G R, Synthesis of carboxymethyl starch co (polyacrylamide/ polyacrylic acid) hydrogel for removing methylene blue dye from aqueous solution, *Int J Biol Macromol*, 269 (2024) 132053.
26 Seera S D K, Kundu D, Gami P, Naik P K & Banerjee T, Synthesis and characterization of xylan-gelatin cross-linked reusable hydrogel for the adsorption of methylene blue, *Carbohydr Polym*, 256 (2021) 117520.
27 Tang Z, Hu X, Ding H, Li Z, Liang R & Sun G, Villi-like poly(acrylic acid) based hydrogel adsorbent with fast and highly efficient methylene blue removing ability, *J Colloid Interface Sci*, 594 (2021) 54.
28 Manu, Kumar D & Gupta R K, Novel formulations of humic acid, lignin, and lignite grafted hydrogels for the slow release of thiamethoxam, *Chem Select*, 9 (2024) e202304939.

29 Pehlivan E & Arslan G, Comparison of adsorption capacity of young brown coals and humic acids prepared from different coal mines in Anatolia, *J Hazard Mater*, 138 (2006) 401.

30 Havelcová M, Mizera J, Sýkorová I & Pekař M, Sorption of metal ions on lignite and the derived humic substances, *J Hazard Mater*, 161 (2009) 559.

31 Zherebtsov S I, Malyshenko N V, Votolin K S & Ismagilov Z R, Sorption of metal cations by lignite and humic acids, *Coke Chem*, 63 (2020) 142.

32 Klučáková M & Pavlíková M, Lignitic humic acids as environmentally-friendly adsorbent for heavy metals, *J Chem*, 2017 (2017) 1.

33 Singh T & Singhal R, Kinetics and thermodynamics of cationic dye adsorption onto dry and swollen hydrogels poly(acrylic acid-sodium acrylate-acrylamide) sodium humate, *Desalin Water Treat*, 53 (2015) 3668.

34 Yu C, Wang F, Zhang C, Fu S & Lucia L A, The synthesis and absorption dynamics of a lignin-based hydrogel for remediation of cationic dye-contaminated effluent, *React Funct Polym*, 106 (2016) 137.

35 Vijayan J G, Prabhu T N & Pal K, Poly(N-isopropyl acrylamide)-co-poly(sodium acrylate) hydrogel for the adsorption of cationic dyes from aqueous solution, *Eur Phys J E*, 46 (2023) 11.

36 Osuchukwu O A, Salihi A, Abdullahi I & Obada D O, Taguchi grey relational optimization of sol-gel derived hydroxyapatite from a novel mix of two natural biowastes for biomedical applications, *Sci Rep*, 12 (2022) 17968.

37 Yuan Z, Wang J, Wang Y, Liu Q, Zhong Y, Wang Y, Li L, Lincoln S F & Guo X, Preparation of a poly(acrylic acid) based hydrogel with fast adsorption rate and high adsorption capacity for the removal of cationic dyes, *RSC Adv*, 9 (2022) 21075.

38 Can M, Investigation of the factors affecting acid blue 256 adsorption from aqueous solutions onto red pine sawdust: equilibrium, kinetics, process design, and spectroscopic analysis, *Desalin Water Treat*, 57 (2016) 5636.

39 Ashmawy A, Mahmoud A, Ali A, Sultan M, Mostafa H, Eldeeb E & Alshukur M, *Egypt J Chem*, 66 (2023) 21. Please provide the title of this reference

40 Aljeboree A M & Alkaim A F, Studying removal of anionic dye by prepared highly adsorbent surface hydrogel nanocomposite as an applicable for aqueous solution, *Sci Rep*, 14 (2024) 9102.

41 Pathak J & Singh P, Adsorptive removal of congo red using organically modified zinc-copper-nickel ternary metal hydroxide: Kinetics, isotherms and adsorption studies, *J Polym Environ*, 31 (2023) 327.

42 Duran S, Şolpan D & Güven O, Synthesis and characterization of acrylamide-acrylic acid hydrogels and adsorption of some textile dyes, *Nucl Instrum Methods Phys Res Sect B: Beam Interact Mater Atoms*, 151 (1999) 196.

43 Pandey S, Do J Y, Kim J & Kang M, Fast and highly efficient removal of dye from aqueous solution using natural locust bean gum based hydrogels as adsorbent, *Int J Biol Macromol*, 143 (2020) 60.